Optimization of Grinding and Wheel Parameters during External Cylindrical Longitudinal Machining of AISI 6150 Alloy Steel Based on Accuracy, Quality and Productivity

Aleksandar Milosevic
Assistant
University of Novi Sad
Faculty of Technical Sciences
Serbia

Vitalii Ivanov
Professor
Sumy State University
Faculty of Technical Systems and Energy
Efficient Technologies
Ukraine

Sanda Simunovic
Assistant
University of Slavonski Brod
Mechanical Engineering Faculty
Croatia

Djordje Vukelic
Professor
University of Novi Sad
Faculty of Technical Sciences
Serbia

In this research, a multi-objective optimization study was conducted on the external cylindrical longitudinal grinding process of AISI 6150 alloy steel. The input variables examined for their influence included wheel speed, workpiece speed, feed, total depth of cut, number of passes, wheel grain size, and wheel porosity. Experimental research was carried out using a custom experimental design based on the I-criterion of optimality. Dimensional deviation was selected to quantify accuracy, surface roughness was used for quality assessment, and material removal rate was employed to measure productivity. The dimensional deviation values ranged from 0.0046 to 0.0144 mm, surface roughness values were between 0.4301 and 3.766 μm, and the material removal rate ranged from 9.375 to 112.5 mm³. Using the experimental findings, an analysis was performed to define the impact of input variables on output variables, and regression equations were developed. The goal was to optimize accuracy, quality, and productivity simultaneously while varying the weighting coefficients in the objective function. The reliability of the model and the optimal values of the variables were validated through confirmation experiments. The obtained absolute errors were acceptable, measuring between 0.0004 to 0.001 mm for dimensional deviation and 0.0102 to 0.0245 μm for surface roughness.

Keywords: *Grinding, dimensional accuracy, surface roughness, material removal rate, optimization.*

1. INTRODUCTION

Grinding is a machining process used to remove material in the form of small chips. It is generally considered a finishing process that achieves high dimensional and geometric accuracy, as well as a high-quality surface finish. As demands for increased productivity and lower costs rise, it is crucial for grinding to be performed more efficiently and in less time [1].

Modelling and optimization play a vital role in controlling the machining processes [2,3], including grinding, to enhance product quality, productivity and cost-effectiveness. However, optimizing the grinding process is complex because it requires consideration of a wide range of input variables. These factors include the characteristics of the workpiece, workpiece speed, wheel diameter, wheel width, wheel speed, feed rate, depth of cut, number of passes, depth of dressing, lead of dressing, grain size, wheel bond type, grinding ratio, and the properties of the cutting fluid, among others [4-6].

The criteria for optimizing grinding operations can vary significantly and may include factors such as dimensional accuracy, surface roughness, residual stresses, hardness, energy consumption, processing time, and overall cost. The optimization problem is further complicated by the non-stationary and non-linear relationships between input and output variables. Additionally, some input variables can only take on discrete values, which extends the duration and increases the cost of research [7,8].

Developing reliable and accurate analytical models for the grinding process is challenging; thus, practitioners often rely heavily on operators' knowledge and experience. Currently, there are no comprehensive grinding models that effectively relate all input and output variables. Furthermore, the optimization objectives may differ depending on the specific application.

It is desirable to create an optimization methodology that is not limited to a particular process or goal. Conventional optimization methods may converge to a local minimum or maximum based on the chosen objective function or diverge when the problem is not clearly defined. As a result, there is a growing interest in optimization methods that are based on artificial intelligence.

In the previous period, various approaches and methods were employed to optimize the cylindrical external grinding process. Rekha et al. [9] investigated the optimization of grinding parameters using Taguchi-based grey relational analysis. They analysed the effects of workpiece speed, longitudinal and transverse feed, and

Received: January 2026, Accepted: February 2026
Correspondence to: Sanda Simunovic
University of Slavonski Brod, Mechanical Engineering Faculty, Slavonski Brod, Croatia
E-mail: ssimunovic@unisb.hr
doi: 10.5937/fme2602199M

coolant flow rate on surface roughness and material removal rate, identifying the optimal settings that balance both outputs. The best results were achieved with a low transverse feed and a high coolant flow rate. Kara et al. [10] examined the influence of grinding wheel type, cryogenic treatment time, and depth of cut on surface roughness. The findings revealed that the best surface roughness was obtained with the Al_2O_3 wheel, a 30-hour cryogenic treatment, and the smallest depth of cut of 100 μm. The most significant parameter affecting the surface roughness was the type of grinding wheel, followed by cryogenic treatment time and depth of cut. Rudrapati et al. [11] employed a combined approach using response surface methodology (RSM) and a simulated annealing (SA) algorithm for modelling and optimizing surface roughness in the cylindrical grinding of stainless steel. Their experiments were designed factorially with input variables such as infeed, longitudinal feed, and workpiece speed. Analysis of variance (ANOVA) indicated that workpiece speed had the greatest impact on surface roughness, while longitudinal feed and parameter interactions also proved significant. Chi et al. [12] developed a simulation model for the surface topography in external cylindrical grinding, which accounted for the trajectory of abrasive grains and their interaction with the workpiece. The model successfully predicted changes in roughness that were consistent with experimental results, providing a foundation for optimizing grinding parameters. Hong et al. [13] focused on cost optimization for the external cylindrical grinding process by determining the optimal grinding wheel diameter for replacement. They analysed seven factors: grinding wheel diameter, grinding wheel width, wheel life, radial grinding wheel wear, total depth of cut, machine tool hourly rate, and grinding wheel cost. The results demonstrated that the initial grinding wheel diameter significantly influenced the timing of its replacement. Panthangi & Naduvinamani [14] optimized cylindrical grinding parameters to minimize surface roughness using the Taguchi method and genetic algorithm (GA). Their findings indicated that material hardness had the greatest influence on surface quality, while depth of cut and workpiece speed had a lesser effect. Trung et al. [15] conducted a multi-objective optimization of the cylindrical grinding process focusing on minimizing surface roughness and maximizing material removal rate (MRR). Among the process parameters studied, cutting speed had the most significant impact on surface roughness, while feed and depth of cut were more crucial for MRR.

Longitudinal cylindrical external grinding represents a specialized area within the broader field of grinding, characterized by unique technical requirements and process features that influence the selection of parameters and overall outcomes. Several studies have focused on optimizing the parameters associated with this type of grinding to better comprehend its distinct effects and identify optimal solutions. Gopan et al. [16] employed an integrated approach combining artificial neural networks (ANN) and GA to predict and optimize external longitudinal cylindrical grinding parameters with the goal of minimizing surface roughness. Their results indicated that a combination of higher wheel speed with lower feed and depth of cut results in improved surface quality. Nguyen et al. [17] conducted a multi-objective optimization of external cylindrical grinding using grey relational analysis. They examined the effects of dressing and feed parameters on both surface roughness and grinding wheel life. The optimal settings significantly enhanced performance, achieving low surface roughness and extended wheel life. In another study, Nguyen [18] carried out experimental analysis and optimization of the external cylindrical grinding process. Utilizing GA, they modelled the influence of parameters such as feed, workpiece speed, depth of cut, and workpiece hardness on surface roughness, cutting forces, and vibrations. The best surface quality and material removal efficiency were achieved with low feed, medium workpiece speed, and small depth of cut. Jadhav et al. [19] investigated the optimization of the cylindrical grinding process to increase MRR. Applying the Taguchi method and grey relational analysis, they discovered that depth of cut had the greatest influence on MRR, whereas cutting speed and feed had a relatively minor impact. Kumar Patel et al. [20] evaluated the effects of grinding wheel speed, depth of cut, workpiece speed, and grinding wheel material and grade on surface roughness. They identified that selecting the appropriate grinding wheel material and grade significantly impacted surface roughness, making these factors the most influential. Alsigar et al. [21] developed a methodology for optimizing external cylindrical grinding with axial feed through mathematical models. These models described the relationship between cutting forces and elastic deformations of the system under unstable conditions, facilitating the automatic calculation of optimal feed rates and the design of control cycles. Tien et al. [22] applied the preference selection index (PSI) method for multi-objective optimization, aiming to minimize surface roughness while maximizing MRR. Their findings indicated that workpiece speed had a negligible effect, while feed and depth of cut were the dominant factors. Rudrapati et al. [23] optimized the parameters of longitudinal cylindrical grinding to minimize vibrations and surface roughness. The varied parameters included infeed, longitudinal feed, and workpiece speed. Using RSM and GA for optimization, they found that infeed significantly influenced vibrations, while surface roughness was primarily impacted by interaction effects and quadratic terms. Gangmei et al. [24] utilized a fuzzy approach to optimize cylindrical grinding, focusing on increasing MRR while maintaining desired surface roughness. Their study demonstrated that this method allows for defining a broader range of suitable parameters rather than a single optimal point, thus facilitating the selection of processing conditions. Giang et al. [25] optimized the dressing parameters to minimize surface roughness. Using the Taguchi method and ANOVA analysis, they determined that the depth of dressing had the most significant effect on roughness, while the depth of coarse dressing and feed were less influential. Ding et al. [26] studied temperature distribution and energy partitioning during cylindrical grinding through finite element modelling and experimental verification. They found that workpiece speed significantly affects the

amount of energy converted into chips, and careful selection of grinding parameters can mitigate the thermal impact on the workpiece. Rekha et al. [27] developed a regression model to predict surface roughness in cylindrical grinding with a minimal number of experiments. They optimized parameters such as workpiece speed, feed, and depth of cut using GA and particle swarm optimization (PSO). The best surface finish was obtained with a combination of high workpiece speed and low feed and depth of cut. Lastly, Neseli et al. [28] applied a combination of the Taguchi method and RSM to optimize the parameters of external cylindrical grinding, aiming to reduce surface roughness and grinding wheel vibrations. They discovered that workpiece speed and depth of cut were the most significant factors, achieving the best surface roughness with a low depth of cut and higher workpiece speed.

Most previous research in external longitudinal cylindrical grinding has primarily concentrated on either minimizing surface roughness or increasing the material removal rate. While these studies have provided valuable insights into specific aspects of the process, few have considered all the key requirements of modern grinding—precision, quality, and productivity—in an integrated manner. Additionally, earlier studies often focused on a limited set of input variables, mainly related to basic machining conditions such as workpiece speed, feed, and depth of cut, while neglecting other significant factors, like grinding wheel characteristics or dressing parameters. Furthermore, many previous works have not adequately addressed the interdependencies between parameters and their simultaneous influence on various output characteristics. This consideration is crucial for industrial applications, where it is essential to find an optimal balance between precision, surface quality, and productivity. The complex and nonlinear relationships between input and output variables further complicate the modelling and optimization process, underscoring the need for a comprehensive approach.

In contrast, this research aims to provide a thorough analysis, modelling, and optimization of the impact of a wide range of grinding parameters and grinding wheel characteristics on the external longitudinal cylindrical grinding of AISI 6150 alloy steel. To reliably identify statistically significant factors, we applied ANOVA, while the accuracy and stability of the developed regression models were assessed using k-fold cross-validation. Special emphasis is placed on three key process parameters: dimensional accuracy, surface quality, and material removal rate. This approach is designed to identify the optimal combination of parameters that achieves high quality and accuracy while simultaneously enhancing productivity, which is critical for modern manufacturing systems.

2. METHODOLOGY

The research methodology is illustrated in Figure 1. The experiments were conducted on workpieces with a diameter of 30 mm and a length of 500 mm, made from AISI 6150 alloy steel, which were machined to an initial surface roughness of $Ra \approx 8.3$ μm. The chemical composition of AISI 6150 alloy steel is listed in Table 1. The mechanical, physical and thermal properties of AISI 6150 alloy steel are outlined in Table 2.

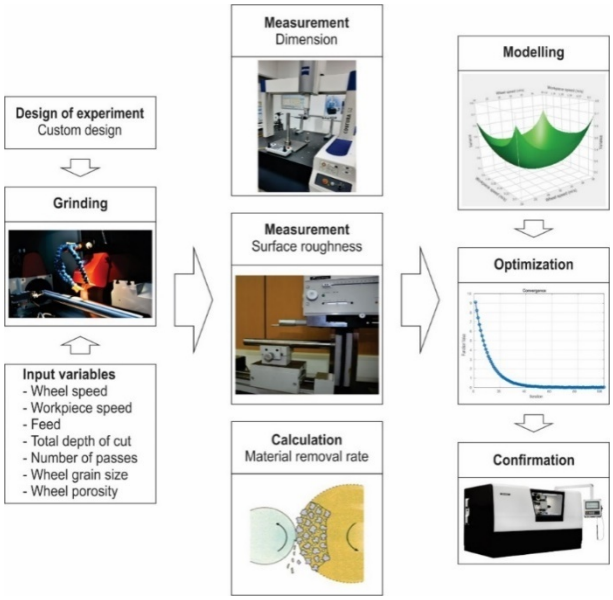

Figure 1. Structure of the research methodology

Table 1. Chemical composition of AISI 6150 alloy steel

Element	Content (%)
Iron, Fe	97.1 - 97.7
Chromium, Cr	0.8 - 1.1
Manganese, Mn	0.7 - 0.9
Carbon, C	0.48 - 0.53
Silicon, Si	0.15 - 0.3
Vanadium, V	≤ 0.15
Sulfur, S	≤ 0.04
Phosphorous, P	≤ 0.035

Table 2. Properties of AISI 6150 alloy steel

Properties	Value
Tensile strength, ultimate	670 MPa
Modulus of elasticity	200 GPa
Shear modulus	80 GPa
Bulk modulus	140 GPa
Poissons ratio	0.29
Brinell Hardness	197
Density	7.85 g/cm^3
Thermal conductivity	46.6 W/mK

External cylindrical longitudinal grinding was performed on a CNC grinding machine. The workpiece, located between centers, was rotated by a driving plate and a grinding dog. The grinding parameters and wheel specifications were selected based on the manufacturer's recommendations for the machine tool and cutting tools. During grinding, the synthetic cutting fluid Syntilo was applied.

For each experiment, a new straight grinding wheel with dimensions of $D \times B \times d = 350 \times 50 \times 127$ mm was utilized. The wheel was made of corundum (98% Al_2O_3) abrasive, had a medium hardness grade, and was bonded with a ceramic type.

During the experimental study, seven input variables were varied, as shown in Table 3. Wheel speed, workpiece speed, feed, total depth of cut, and wheel grain size are considered continuous variables. In contrast, the number of passes and porosity are classified as categorical variables with discrete levels.

Table 3. Input variable levels

Parameter	Level		
	Min.	Mean	Max.
Wheel speed, v_c (m/s)	25	30	35
Workpiece speed, v_w (m/s)	0.2	0.25	0.3
Feed, f (mm/rev)	12.5	18.75	25
Total depth of cut, Δ (mm)	0.12	0.24	0.36
Number of passes, i	4	6	8
Wheel grain size, WGS	Coarse	Medium	Fine
Wheel porosity, WP	Dense	Medium	Porous

Once the experiments are completed, measurements are taken and calculations are performed.

All measurements of dimensions and surface roughness were conducted under controlled microclimatic conditions, maintaining a temperature of 20±1 °C. To minimize errors, each measurement was taken ten times.

The dimensions were assessed using a Carl Zeiss coordinate measuring machine. A measuring probe with a length of 70 mm and a ball diameter of 5 mm was employed, utilizing a point-by-point measurement strategy.

The diameter of the workpiece is measured both before and after grinding, and then the measurements are used for calculations. The calculation of dimensional accuracy (Δd) is performed using the following equation:

$$\Delta d = \left| d_{2n} - d_{2m} \right| \tag{1}$$

where d_{2n} is the required - nominal value of the diameter after grinding and d_{2m} is the measured value of the diameter after grinding.

The required nominal value of the diameter after grinding is determined using the equation:

$$\Delta d_{2n} = d_{1m} - 2 \cdot \Delta \tag{2}$$

where d_{1m} is the measured diameter value before grinding and Δ is the total depth of cut.

By substituting equation (2) into equation (1), we derive the following equation to calculate dimensional accuracy:

$$\Delta d = \left| d_{1m} - 2 \cdot \Delta - d_{2m} \right| \tag{3}$$

Surface roughness (Ra) was measured using a Talysurf device. The measurements were taken with a sampling length of 0.8 mm and an evaluation length of 4 mm, employing a Gaussian filter.

Finally, MRR is the output variable that is calculated. For cylindrical grinding with longitudinal feed, the MRR can be computed using the equation:

$$MRR = f \cdot a_p \cdot B = f \cdot \frac{\Delta}{i} \cdot B = \frac{f \cdot \Delta \cdot B}{i} \tag{4}$$

where f is feed, a_p is depth of cut, B is wheel width, Δ is total depth of cut and i is number of passes.

The experimental plan was developed using the custom design of experiment in JMP software, applying the I-optimality criterion. This criterion focuses on minimizing the average prediction variance across the entire experimental domain, which is essential for obtaining accurate and reliable estimates of output variables—crucial for subsequent optimization and process control.

During the design definition, previously established input and output variables were taken into account, based on which an a priori model was constructed that includes main effects, quadratic effects, and two-factor interactions, aiming to identify and quantify the influence of input on output variables. The number of experimental runs was determined through careful evaluation. This evaluation involved power analysis, taking into account the significance level, expected effect sizes, and measurement variability. Figure 2 shows the results of the power analysis for different numbers of experimental runs (54, 80, 108 and 144). The analysis evaluates the statistical power for detecting the effects of model terms, including main effects, interactions, and quadratic terms. As shown, a higher number of runs leads to a significant increase in power across almost all terms, with 108 and 144 runs ensuring power values above the conventional threshold of 0.8. It was concluded that 108 experimental runs would provide sufficient data to reliably detect statistically significant effects. Additionally, the uniformity of the run distribution within the experimental space was carefully assessed, ensuring stable and precise model estimates, thereby confirming the validity and efficiency of the chosen design.

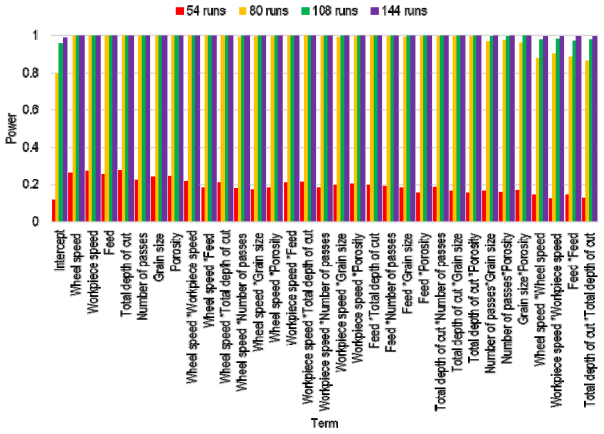

Figure 2. Power analysis for different numbers of experimental runs

Based on the collected experimental data, process modelling was performed. Regression models were used to link the input process parameters with the measured output variables, enabling the identification of key factors and their mutual interactions. These models were further validated through statistical tests and residual analysis, confirming their capability to accurately describe the process behaviour within the defined experimental domain.

Using the developed regression models, multi-objective optimization was conducted. Multi-objective optimization is particularly suitable for addressing complex problems where individual objectives may conflict. The optimization aimed to simultaneously minimize Δd and Ra, while maximizing MRR. The objective function can be expressed as:

$$F_c = w_{\Delta d} \cdot \min x_{\Delta d} + w_{Ra} \cdot \min x_{\Delta d} + w_{MRR} \cdot \max x_{MRR} \tag{5}$$

In this equation, $w_{\Delta d}$, w_{Ra}, w_{MRR} represent the weighting coefficients, while $x_{\Delta d}$, x_{Ra}, x_{MRR} denote the normalized values of the output variables for the process.

These normalized values are calculated using the following formula:

$$x_y = \frac{y - y_{\min}}{y_{\max} - y_{\min}} \; y = \Delta d, Ra, MRR \tag{6}$$

Based on the characteristics of the technological equipment and the conditions of the experimental research, the following constraints are defined:

- wheel speed, $v_c = 25 \le v_c \le v_c = 35$ (m/s), continuous input variable,
- workpiece speed, $v_w = 0.2 \le v_w \le v_w = 0.3$ (m/s), continuous input variable,
- feed, $f = 12.5 \le f \le f = 25$ (mm/rev), continuous input variable,
- total depth of cut, $\Delta = 0.12 \le \Delta \le \Delta = 0.36$ (mm), continuous input variable,
- number of passes, $i = 4 \le i \le i = 8$, continuous input variable,
- wheel grain size, $WGS = 24 \le WGS \le WGS = 80$, discrete input variable,
- wheel porosity, $WP = 4 \le WP \le WP = 10$, discrete input variable.

Modelling and optimization performance is assessed through confirmation experiments and by calculating absolute errors:

$$AE_x = \left| x_{i\text{predicted value}} - x_{i\text{measured value}} \right| \tag{7}$$

3. RESULTS

3.1 Results of the Experimental Research

Table 4 presents the results of measurements and calculations for various combinations of input variables. Dimensions and surface roughness were measured ten times, and the table shows the mean values rounded to four decimal places.

Table 4. Results of the experimental research

No.	v_c(m/s)	v_w(m/s)	f(mm/rev)	Δ(mm)	i	WGS	WP	Δd(mm)	Ra(μm)	MRR(mm^3)
1	25	0.2	25	0.36	8	Coarse	Dense	0.0066	3.6374	56.25
2	30	0.25	18.75	0.24	8	Coarse	Medium	0.0075	3.3920	28.125
3	35	0.25	25	0.36	4	Coarse	Porous	0.0131	3.4388	112.5
4	30	0.3	12.5	0.12	6	Medium	Porous	0.0101	1.4413	12.5
5	25	0.3	12.5	0.12	8	Coarse	Medium	0.0078	3.4388	9.375
6	35	0.2	12.5	0.36	6	Medium	Porous	0.0107	1.3678	37.5
7	35	0.25	12.5	0.12	6	Coarse	Medium	0.0094	3.1816	12.5
8	30	0.3	18.75	0.12	6	Medium	Medium	0.0089	1.5505	18.75
9	25	0.2	12.5	0.12	6	Coarse	Dense	0.0056	3.3686	12.5
10	30	0.2	25	0.12	4	Medium	Dense	0.0068	1.5862	37.5
11	25	0.2	25	0.36	4	Fine	Porous	0.0079	0.5062	112.5
12	35	0.25	18.75	0.36	6	Medium	Medium	0.0104	1.5191	56.25
13	25	0.3	18.75	0.36	8	Medium	Medium	0.0085	1.6293	42.1875
14	30	0.3	25	0.36	8	Coarse	Porous	0.0116	3.5439	56.25
15	35	0.3	25	0.36	6	Fine	Porous	0.0133	0.4981	75
16	30	0.2	18.75	0.36	6	Coarse	Porous	0.0091	3.2985	56.25
17	25	0.3	25	0.36	4	Fine	Medium	0.0094	0.5620	112.5
18	25	0.3	12.5	0.24	4	Medium	Medium	0.0089	1.5904	37.5
19	25	0.2	25	0.12	8	Medium	Porous	0.0062	1.4980	18.75
20	35	0.2	25	0.36	8	Medium	Dense	0.0095	1.5705	56.25
21	35	0.3	12.5	0.24	8	Medium	Porous	0.0124	1.4098	18.75
22	25	0.2	12.5	0.36	8	Fine	Medium	0.0049	0.4681	28.125
23	35	0.2	18.75	0.24	8	Fine	Dense	0.0083	0.5060	28.125
24	25	0.2	18.75	0.24	6	Medium	Dense	0.0059	1.5946	37.5
25	25	0.2	12.5	0.12	4	Coarse	Medium	0.0054	3.2985	18.75
26	25	0.3	25	0.12	4	Coarse	Dense	0.0089	3.7660	37.5
27	35	0.2	18.75	0.24	4	Medium	Medium	0.0094	1.4772	56.25
28	25	0.2	12.5	0.12	6	Fine	Porous	0.0056	0.4301	12.5
29	30	0.25	18.75	0.24	6	Fine	Porous	0.0083	0.4820	37.5
30	25	0.2	25	0.36	6	Fine	Dense	0.0062	0.5461	75
31	25	0.3	25	0.36	4	Medium	Dense	0.0104	1.7752	112.5
32	35	0.25	18.75	0.12	4	Coarse	Dense	0.0102	3.3921	28.125
33	25	0.2	25	0.12	4	Fine	Dense	0.0051	0.5302	37.5
34	35	0.25	12.5	0.12	4	Medium	Dense	0.0096	1.4771	18.75
35	30	0.25	18.75	0.24	8	Coarse	Medium	0.0076	3.3922	28.125
36	35	0.3	18.75	0.12	6	Coarse	Porous	0.0128	3.2751	18.75
37	35	0.2	25	0.12	6	Fine	Medium	0.0077	0.5020	25
38	30	0.3	12.5	0.12	4	Coarse	Porous	0.0108	3.2985	18.75
39	30	0.25	12.5	0.36	4	Medium	Porous	0.0103	1.4728	56.25
40	35	0.2	25	0.36	8	Coarse	Medium	0.0094	3.3569	56.25
41	25	0.3	12.5	0.36	4	Fine	Porous	0.0105	0.4900	56.25
42	25	0.3	12.5	0.36	6	Coarse	Porous	0.0107	3.4855	37.5
43	25	0.2	12.5	0.36	6	Coarse	Medium	0.0065	3.3921	37.5
44	25	0.25	18.75	0.36	4	Coarse	Medium	0.0083	3.6258	84.375

45	25	0.25	25	0.24	4	Coarse	Porous	0.0091	3.5790	75
46	25	0.25	12.5	0.24	8	Coarse	Porous	0.0077	3.2985	18.75
47	30	0.2	18.75	0.24	4	Medium	Porous	0.0087	1.4644	56.25
48	35	0.3	18.75	0.36	4	Medium	Porous	0.0144	1.5274	84.375
49	35	0.3	12.5	0.36	6	Medium	Dense	0.0127	1.5611	37.5
50	35	0.3	25	0.24	8	Medium	Porous	0.0127	1.5192	37.5
51	35	0.3	25	0.36	8	Fine	Medium	0.0113	0.5161	56.25
52	30	0.2	25	0.36	4	Medium	Medium	0.0082	1.5946	112.5
53	35	0.3	12.5	0.36	4	Coarse	Medium	0.0134	3.4388	56.25
54	35	0.2	25	0.12	6	Medium	Porous	0.0096	1.4245	25
55	30	0.25	18.75	0.24	8	Medium	Dense	0.0076	1.5736	28.125
56	30	0.25	18.75	0.24	6	Fine	Porous	0.0085	0.4822	37.5
57	25	0.2	12.5	0.36	8	Medium	Porous	0.0069	1.4361	28.125
58	35	0.3	12.5	0.12	8	Fine	Medium	0.0102	0.4501	9.375
59	30	0.25	18.75	0.24	6	Medium	Dense	0.0080	1.5946	37.5
60	30	0.2	12.5	0.36	4	Coarse	Dense	0.0089	3.4388	56.25
61	25	0.2	25	0.36	6	Medium	Medium	0.0063	1.6156	75
62	35	0.3	25	0.12	6	Medium	Dense	0.0116	1.6177	25
63	35	0.2	12.5	0.12	8	Medium	Medium	0.0078	1.3594	9.375
64	25	0.3	18.75	0.36	6	Coarse	Dense	0.0099	3.7660	56.25
65	25	0.25	12.5	0.24	4	Fine	Dense	0.0069	0.5141	37.5
66	30	0.25	12.5	0.36	8	Medium	Medium	0.0076	1.4907	28.125
67	35	0.3	12.5	0.12	6	Fine	Dense	0.0108	0.4781	12.5
68	25	0.25	12.5	0.36	8	Fine	Dense	0.0064	0.5081	28.125
69	30	0.25	12.5	0.24	6	Coarse	Dense	0.0083	3.4388	25
70	25	0.25	18.75	0.12	4	Fine	Medium	0.0055	0.4981	28.125
71	30	0.25	18.75	0.24	4	Fine	Medium	0.0077	0.5140	56.25
72	25	0.3	25	0.36	6	Medium	Porous	0.0105	1.6450	75
73	35	0.3	25	0.24	6	Coarse	Medium	0.0121	3.5323	50
74	25	0.2	12.5	0.12	6	Medium	Medium	0.0047	1.4539	12.5
75	35	0.2	12.5	0.36	6	Fine	Dense	0.0093	0.4982	37.5
76	35	0.25	12.5	0.36	8	Fine	Porous	0.0106	0.4441	28.125
77	35	0.3	25	0.12	4	Fine	Porous	0.0122	0.4821	37.5
78	35	0.2	25	0.12	4	Coarse	Medium	0.0089	3.2985	37.5
79	35	0.2	18.75	0.12	8	Coarse	Porous	0.0098	3.0648	14.0625
80	30	0.25	18.75	0.36	6	Fine	Medium	0.0077	0.5140	56.25
81	35	0.2	12.5	0.24	8	Coarse	Dense	0.0091	3.2050	18.75
82	25	0.3	25	0.12	6	Fine	Dense	0.0078	0.5580	25
83	25	0.2	25	0.12	8	Coarse	Dense	0.0057	3.5323	18.75
84	25	0.3	25	0.12	6	Coarse	Medium	0.0083	3.6491	25
85	30	0.2	12.5	0.12	8	Fine	Dense	0.0056	0.4901	9.375
86	25	0.25	18.75	0.12	4	Medium	Porous	0.0074	1.5064	28.125
87	35	0.3	12.5	0.36	8	Coarse	Dense	0.0125	3.4504	28.125
88	35	0.3	25	0.12	8	Coarse	Dense	0.0118	3.5323	18.75
89	25	0.3	18.75	0.12	8	Fine	Porous	0.0084	0.4820	14.0625
90	30	0.3	25	0.24	8	Fine	Dense	0.0091	0.5461	37.5
91	25	0.2	25	0.12	6	Coarse	Porous	0.0068	3.3686	25
92	35	0.3	25	0.12	4	Medium	Medium	0.0113	1.5736	37.5
93	30	0.3	18.75	0.24	4	Coarse	Dense	0.0111	3.6725	56.25
94	25	0.25	25	0.12	8	Medium	Medium	0.0057	1.5946	18.75
95	30	0.25	25	0.12	8	Fine	Porous	0.0078	0.4901	18.75
96	30	0.25	25	0.24	6	Coarse	Dense	0.0086	3.6258	50
97	25	0.3	12.5	0.12	8	Medium	Dense	0.0079	1.5821	9.375
98	30	0.3	18.75	0.24	4	Fine	Dense	0.0101	0.5382	56.25
99	35	0.2	25	0.36	8	Fine	Porous	0.0099	0.4920	56.25
100	25	0.2	25	0.24	8	Fine	Medium	0.0046	0.5061	37.5
101	25	0.3	18.75	0.36	8	Fine	Porous	0.0093	0.5000	42.1875
102	35	0.25	25	0.36	4	Fine	Dense	0.0112	0.5542	112.5
103	35	0.2	25	0.36	6	Coarse	Dense	0.0105	3.4855	75
104	35	0.2	12.5	0.12	4	Fine	Porous	0.0091	0.4342	18.75
105	25	0.3	12.5	0.24	6	Fine	Medium	0.0076	0.4980	25
106	35	0.2	12.5	0.24	4	Coarse	Porous	0.0111	3.1115	37.5
107	35	0.2	12.5	0.36	4	Fine	Medium	0.0095	0.4821	56.25
108	25	0.2	12.5	0.36	4	Medium	Dense	0.0073	1.5821	56.25

The results obtained demonstrate the ability to control the output variables across extensive ranges:

- For Δd, the values range from 0.0046 mm to 0.0144 mm, resulting in a maximum-to-minimum ratio of 3.1304.
- For *Ra*, the values span from 0.4301 μm to 3.766 μm, yielding a maximum-to-minimum ratio of 8.7561.
- For *MRR*, the values extend from 9.375 mm³ to 112.5 mm³, which gives a maximum-to-minimum ratio of 12.

3.2 Results of Modelling

The experimental results were analysed statistically using regression analysis with the least squares fit method. A model was developed that incorporates all the main effects of the input variables, their interactions, and quadratic terms. This approach allows for a comprehensive understanding of the nonlinear and combined influences of the factors on the output variables. Multiple regression analysis was performed simultaneously for two responses: surface roughness and dimensional deviation. This enabled the identification of factors that significantly affect both responses. During the analysis, a 95% confidence interval was established, ensuring a high level of reliability in estimating the regression coefficients and in drawing conclusions from the resulting models.

Table 5 presents the estimated effects of the factors included in the model, emphasizing their statistical significance, as indicated by LogWorth values. LogWorth is a transformation of the p-value (−log10 (p)), which makes it easier to visually compare the significance of individual effects. Higher LogWorth values correspond to lower p-values, indicating a stronger statistical influence of a factor on the response variable. The effects are ranked according to their statistical strength, which helps identify the important factors in the model. Factors with p-values below 0.05 are considered statistically significant and are included in the final model, while those with higher p-values and insignificant contributions are excluded. This method results in a simpler, more efficient, and robust model that highlights only the effects that genuinely influence the behaviour of the studied system.

Table 5. Effect summary

Source	LogWorth	p-value
WGS	177.959	0.00000
v_c	109.027	0.00000
v_w	104.242	0.00000
Δ	79.995	0.00000
WP	78.061	0.00000
f	71.572	0.00000
i	64.180	0.00000
v_c× *WGS*	55.458	0.00000
v_w× *WGS*	55.250	0.00000
f× *WGS*	49.670	0.00000
WGS× *WP*	45.695	0.00000
v_w× v_w	45.048	0.00000
v_c× v_c	43.656	0.00000
Δ× *WGS*	38.360	0.00000
Δ×*i*	37.048	0.00000
i× *WGS*	21.838	0.00000

ANOVA was conducted to assess the statistical significance of the developed regression models for predicting Δd and *Ra*. This analysis helps determine whether variations in the output variables can be attributed to the factors defined in the experimental design. In other words, it evaluates whether the model significantly improves the explanation of the data compared to random error. The results of the ANOVA are presented in Table 6.

Table 6. Analysis of variance

Source	DF	Δd			
		Sum of Squares	Mean Square	F Ratio	Prob>F
Model	30	0.00050794	0.000017	3871.824	<.0001
Error	77	0.00000034	4.373e-9		
C.Total	107	0.00050827			
		Ra			
Model	30	163.31286	5.44376	110680.4	<.0001
Error	77	0.00379	4.918e-5		
C.Total	107	163.31665			

An additional evaluation of the regression model's quality is presented in Table 7, through the fundamental model fit metrics.

Table 7. Summary of fit

Parameter	Δd	*Ra*
RSquare	0.999338	0.999977
RSquare Adj	0.999079	0.999968
Root Mean Square Error	6.613e-5	0.007013
Mean of Response	0.008927	1.840204

To further verify and assess the robustness of the developed regression models, a k-fold cross-validation (k=10) was conducted. In each iteration, the model was trained on 9 out of the 10 data subsets, while the remaining subset was reserved for independent validation. This process was repeated ten times, ensuring that each subset was used exactly once as the test set. The validation results were analysed using one-way ANOVA on the residuals for the output responses Δd and *Ra*. Visual confirmation of model stability was provided through box plot diagrams of the predicted values (Predicted Δd by validation and Predicted *Ra* by validation). These diagrams illustrate a consistent and uniform distribution of estimates between the training and test sets. Figure 3 shows the one-way ANOVA of the residuals for Δd and *Ra* across the folds, indicating that the mean residual values for both parameters are similar in all folds, with no significant deviations in distribution.

Table 8 presents a summary of the fit for the one-way ANOVA of residuals for *Ra* and Δd, organized by validation folds.

Table 9 displays the ANOVA table for the one-way ANOVA test, which evaluates the statistical significance of differences in the means of residuals across the validation groups.

The regression equations (8,9) for dimensional deviation and surface roughness were derived from statistical analysis.

Following the regression analysis, an additional evaluation of the influence of individual input variables on the responses Δd and *Ra* was performed using the prediction profiler (Figure 4).

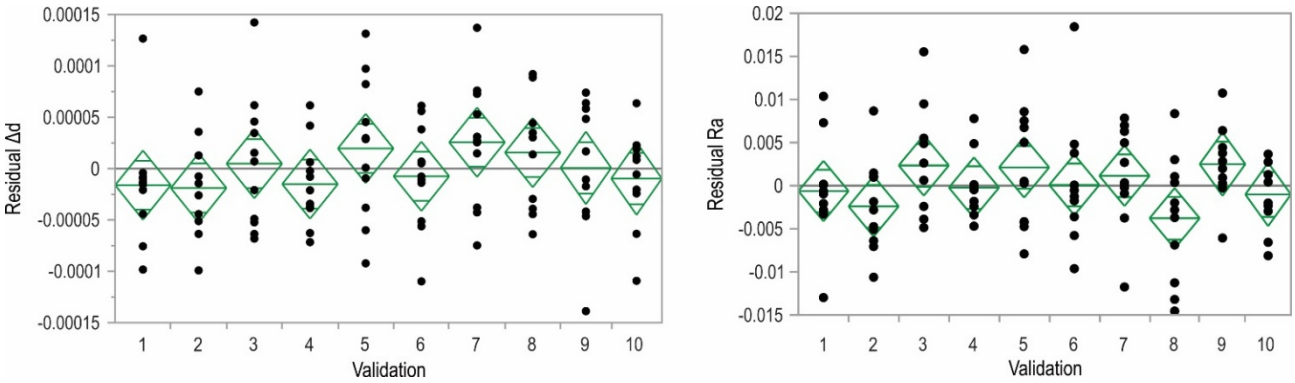

Figure 3. One-way ANOVA of the residuals for Δd and Ra

$$
\begin{aligned}
\Delta d = {} & 0.0082218 + 0.0016364 * \frac{v_c - 30}{5} + 0.0014309 * \frac{v_w - 0.25}{0.05} + 0.0001181 * \frac{f - 18.75}{6.25} + 0.006868 * \frac{\Delta - 0.24}{0.12} \\
& + Match(i) \begin{pmatrix} "4" \to & 0.0004908 \\ "6" \to & -0.0000555 \\ "8" \to & -0.0004354 \\ else \to & . \end{pmatrix} + Match(\mathrm{WGS}) \begin{pmatrix} "Coarse" \to & 0.0004653 \\ "Medium" \to & 0.0000320 \\ "Fine" \to & -0.0004973 \\ else \to & . \end{pmatrix} + + Match(\mathrm{WP}) \begin{pmatrix} "Dense" \to & 0.0001508 \\ "Medium" \to & -0.0006241 \\ "Porous" \to & 0.0007749 \\ else \to & . \end{pmatrix} \\
& + \left(\frac{v_c - 30}{5} \right) * Match(\mathrm{WGS}) \begin{pmatrix} "Coarse" \to & -0.0000023 \\ "Medium" \to & -0.0000089 \\ "Fine" \to & 0.0000112 \\ else \to & . \end{pmatrix} + \left(\frac{v_c - 25}{0.05} \right) * Match(\mathrm{WGS}) \begin{pmatrix} "Coarse" \to & -0.0000046 \\ "Medium" \to & -0.0000065 \\ "Fine" \to & 0.0000111 \\ else \to & . \end{pmatrix} \\
& + \left(\frac{f - 18.75}{6.25} \right) * Match(\mathrm{WGS}) \begin{pmatrix} "Coarse" \to & 0.0000126 \\ "Medium" \to & -0.0000052 \\ "Fine" \to & -0.0000074 \\ else \to & . \end{pmatrix} + \left(\frac{\Delta - 0.24}{0.12} \right) * Match(\mathrm{WGS}) \begin{pmatrix} "4" \to & 0.0002445 \\ "6" \to & -0.0000082 \\ "8" \to & 0.0000044 \\ else \to & . \end{pmatrix} + + \left(\frac{\Delta - 0.24}{0.12} \right) \\
& * Match(\mathrm{WGS}) \begin{pmatrix} "Coarse" \to & 0.0000001 \\ "Medium" \to & 0.0000065 \\ "Fine" \to & 0.0000065 \\ else \to & . \end{pmatrix} + Match(i) \begin{pmatrix} "4" \to & Match(\mathrm{WGS}) \begin{pmatrix} "4" \to & 0.0002445 \\ "6" \to & -0.0000298 \\ "8" \to & -0.0002147 \\ else \to & . \end{pmatrix} \\ "6" \to & Match(\mathrm{WGS}) \begin{pmatrix} "Coarse" \to & -0.0000004 \\ "Medium" \to & 0.0000051 \\ "Fine" \to & -0.0000046 \\ else \to & . \end{pmatrix} \\ "8" \to & Match(\mathrm{WGS}) \begin{pmatrix} "Coarse" \to & -0.0000122 \\ "Medium" \to & 0.0000031 \\ "Fine" \to & -0.0000090 \\ else \to & . \end{pmatrix} \\ else \to & ... \end{pmatrix} \\
& + Match(\mathrm{WGS}) \begin{pmatrix} "Coarse" \to & Match(\mathrm{WGS}) \begin{pmatrix} "Dense" \to & -0.0000033 \\ "Medium" \to & -0.0000163 \\ "Porous" \to & 0.0000196 \\ else \to & . \end{pmatrix} \\ "Medium" \to & Match(\mathrm{WGS}) \begin{pmatrix} "Dense" \to & -0.0000108 \\ "Medium" \to & 0.0000299 \\ "Porous" \to & -0.0000191 \\ else \to & . \end{pmatrix} \\ "Fine" \to & Match(\mathrm{WGS}) \begin{pmatrix} "Dense" \to & 0.0000141 \\ "Medium" \to & -0.0000135 \\ "Porous" \to & -0.0000006 \\ else \to & . \end{pmatrix} \\ else \to & ... \end{pmatrix} + \left(\frac{\left(\frac{v_c - 30}{5} \right) * v_c - 30}{5} \right) * (0.0004868) \\
& + \left(\frac{\left(\frac{v_w - 0.25}{0.05} \right) * v_w - 0.25}{0.05} \right) * (0.0004949)
\end{aligned}
\tag{8}
$$

$$
\begin{aligned}
Ra = {} & 1.8249302 - 0.0475777 * \frac{v_c - 30}{5} + 0.0476175 * \frac{v_w - 0.25}{0.05} + 0.0569375 * \frac{f - 18.75}{6.25} + 0.0325831 * \frac{\Delta - 0.24}{0.12} \\
& + Match(i) \begin{pmatrix} "4" \to & 0.0194236 \\ "6" \to & -0.0006358 \\ "8" \to & -0.0187877 \\ else \to & . \end{pmatrix} + Match(\mathrm{WGS}) \begin{pmatrix} "Coarse" \to & 1.6090973 \\ "Medium" \to & -0.2856175 \\ "Fine" \to & -1.3234798 \\ else \to & . \end{pmatrix} + Match(\mathrm{WP}) \begin{pmatrix} "Dense" \to & 0.0572879 \\ "Medium" \to & -0.0004401 \\ "Porous" \to & -0.0568479 \\ else \to & . \end{pmatrix} \\
& + \left(\frac{v_c - 30}{5}\right) * Match(\mathrm{WGS}) \begin{pmatrix} "Coarse" \to & -0.0454053 \\ "Medium" \to & 0.0054705 \\ "Fine" \to & 0.0399347 \\ else \to & . \end{pmatrix} + \left(\frac{v_w - 25}{0.05}\right) * Match(\mathrm{WGS}) \begin{pmatrix} "Coarse" \to & 0.0463004 \\ "Medium" \to & -0.0062999 \\ "Fine" \to & -0.0400004 \\ else \to & . \end{pmatrix} \\
& + \left(\frac{f - 18.75}{6.25}\right) * Match(\mathrm{WGS}) \begin{pmatrix} "Coarse" \to & 0.0373553 \\ "Medium" \to & -0.0025653 \\ "Fine" \to & -0.0347899 \\ else \to & . \end{pmatrix} + \left(\frac{\Delta - 0.24}{0.12}\right) * Match(\mathrm{WGS}) \begin{pmatrix} "4" \to & 0.0062383 \\ "6" \to & -0.0011160 \\ "8" \to & 0.0051223 \\ else \to & . \end{pmatrix} + + \left(\frac{\Delta - 0.24}{0.12}\right) \\
& * Match(\mathrm{WGS}) \begin{pmatrix} "Coarse" \to & 0.0277982 \\ "Medium" \to & -0.0055673 \\ "Fine" \to & -0.0222309 \\ else \to & . \end{pmatrix} + Match(i) \begin{pmatrix} "4" \to & Match(\mathrm{WGS}) \begin{pmatrix} "Coarse" \to & 0.0171965 \\ "Medium" \to & -0.0033519 \\ "Fine" \to & -0.0138446 \\ else \to & . \end{pmatrix} \\ "6" \to & Match(\mathrm{WGS}) \begin{pmatrix} "Coarse" \to & -0.0005705 \\ "Medium" \to & -0.0000171 \\ "Fine" \to & -0.0005534 \\ else \to & . \end{pmatrix} \\ "8" \to & Match(\mathrm{WGS}) \begin{pmatrix} "Coarse" \to & -0.0166261 \\ "Medium" \to & 0.0033349 \\ "Fine" \to & 0.0132912 \\ else \to & . \end{pmatrix} \\ else \to & ... \end{pmatrix} \\
& + Match(\mathrm{WGS}) \begin{pmatrix} "Coarse" \to & Match(\mathrm{WGS}) \begin{pmatrix} "Dense" \to & 0.0367911 \\ "Medium" \to & -0.0014262 \\ "Porous" \to & -0.0353648 \\ else \to & . \end{pmatrix} \\ "Medium" \to & Match(\mathrm{WGS}) \begin{pmatrix} "Dense" \to & -0.0029713 \\ "Medium" \to & 0.0013156 \\ "Porous" \to & 0.0016557 \\ else \to & . \end{pmatrix} \\ "Fine" \to & Match(\mathrm{WGS}) \begin{pmatrix} "Dense" \to & -0.0338198 \\ "Medium" \to & 0.0001106 \\ "Porous" \to & 0.0337091 \\ else \to & . \end{pmatrix} \\ else \to & ... \end{pmatrix} + \left(\frac{\left(\frac{v_c - 30}{5}\right) * v_c - 30}{5}\right) * (-0.0025002) \\
& + \left(\frac{\left(\frac{v_w - 0.25}{0.05}\right) * v_w - 0.25}{0.05}\right) * (-0.0011718)
\end{aligned}
\tag{9}
$$

Table 8. Summary of fit for one-way ANOVA of residuals for Δ*d* and *Ra*

Parameter	Rsquare	Rsquare Adj	Root Mean Square Error	Mean of Response
Δ*d*	0.0750	–0.0100	5.638×10^{-5}	-6.5×10^{-19}
Ra	0.1117	0.0301	0.005859	2.63×10^{-17}

Table 9. ANOVA results for one-way ANOVA of residuals for Δ*d* and *Ra*

Parameter	Source	DF	Sum of Squares	Mean Square	F Ratio	Prob > F
Δ*d*	Validation	9	2.52509×10^{-8}	2.8057×10^{-9}	0.8828	0.5434
	Error	98	3.11464×10^{-7}	3.1782 × 10-9		
	C. Total	107	3.36715×10^{-7}			
Ra	Validation	9	0.00042294	0.0000470	1.3689	0.2127
	Error	98	0.00336427	0.0000343		
	C. Total	107	0.00378721			

This diagram visually illustrates the changes in each response concerning a single input variable, while keeping all other factors constant. The slope of the lines in the diagram indicates the strength of influence: steeper lines indicate a more significant effect, while gently sloped or horizontal lines suggest a weaker impact from the variable. For the *Ra* response, the grain size factor demonstrated the most significant influence, whereas the other factors had notably smaller effects. Conversely, for the Δ*d* response, the feed parameter exhibited the least influence, and the other input variables had approximately equal and consistent impacts. The prediction profiler also aids in visually identifying optimal input values aimed at achieving the desired output characteristics. Consequently, the results obtained serve as a valuable foundation for further multi-objective process optimization.

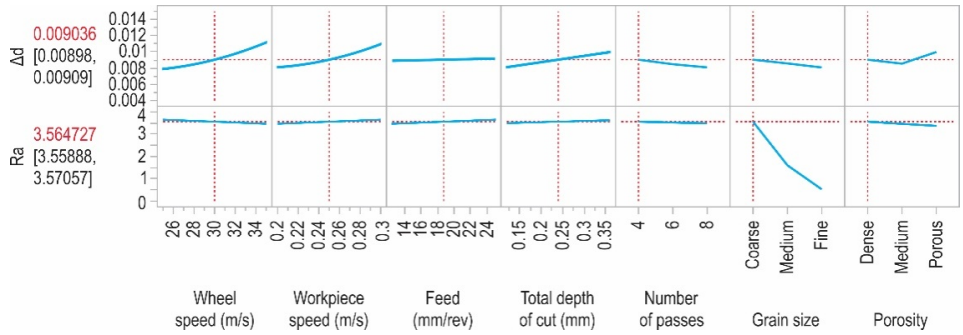

Figure 4. Prediction profilers

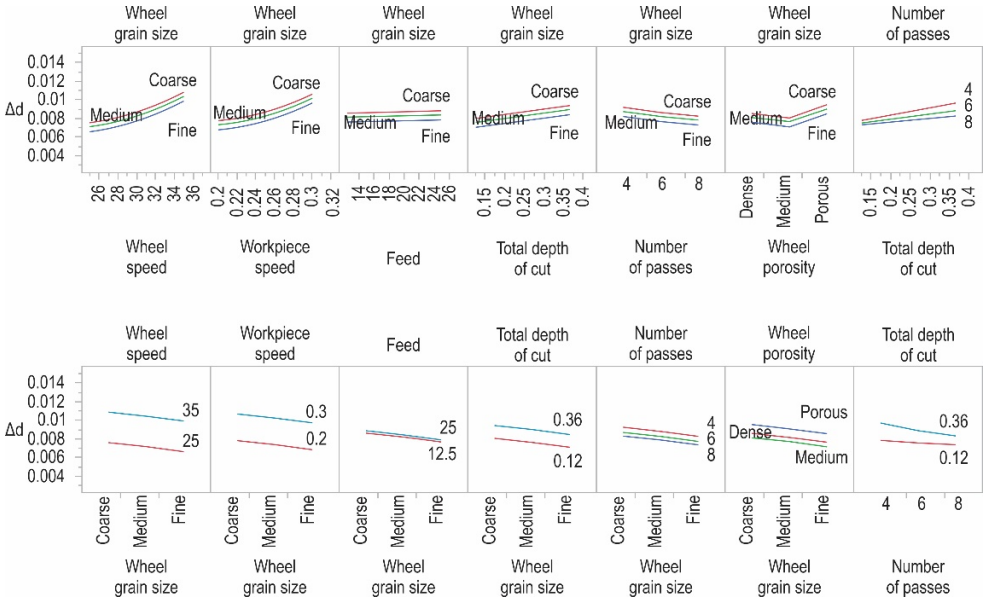

Figure 5. Interaction plots for Δ*d*

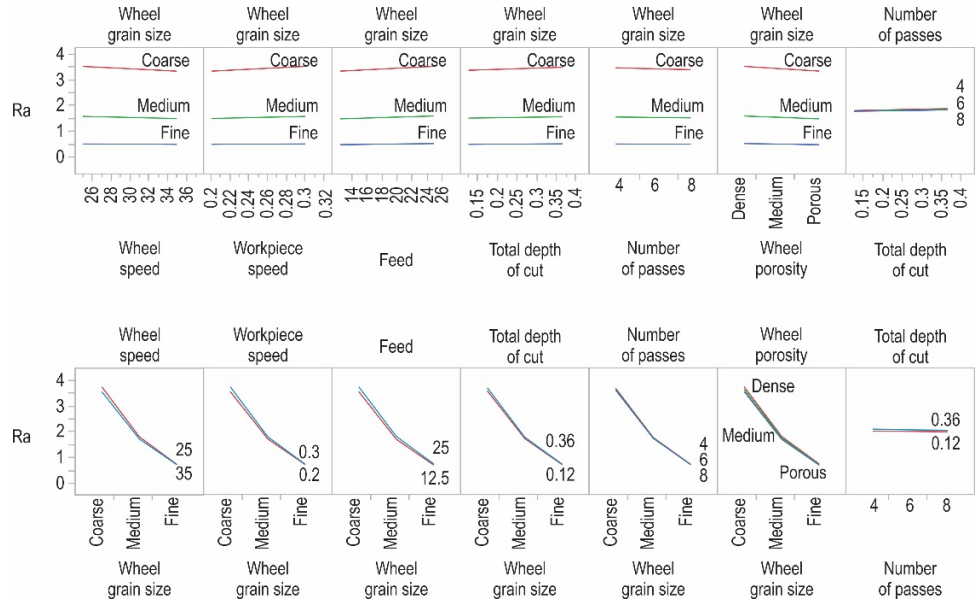

Figure 6. Interaction plots for *Ra*

In addition to analysing the individual effects of input variables on output variables, an interaction ana–lysis was conducted using interaction profiler diagrams for the responses Δd and Ra. The diagrams depicting statistically significant interactions for Δd and Ra are shown in Figures 5 and 6. These diagrams offer insights into how the effect of one factor changes depending on the level of another factor, highlighting interactions that may not be apparent through a focus on main effects alone. The presence of nonlinear or intersecting lines signifies a significant interaction; the more pronounced the curvature or the greater the separation between the lines, the stronger the combined influence of the interacting factors on the observed responses.

3.3 Results of Optimization

A GA was employed to tackle the optimization prob–lem. This heuristic optimization method functions as a directed random search that explores the solution space in search of the global optimum. One of the strengths of genetic algorithms is their ability to identify the global optimum in a space characterized by multiple local extrema. The optimization of the specified criterion was carried out using MATLAB software, specifically the Optimization Toolbox module. The genetic algorithm was configured with a population size of 100 individuals, ensuring suf–ficient diversity among candidates to effectively explore the solution space. The maximum number of generations was set to 50, defining the total iterations during which the algorithm evolves the population. Default values for crossover and mutation probabilities were used, which facilitate the combination of traits from parent individuals and introduce variations. This approach helps maintain population diversity and prevents the algorithm from becoming trapped in local minima.

During the multi-objective optimization process, four cases were examined:

- All output variables are assigned equal importance ($w_{\Delta d} = w_{Ra} = w_{MRR}$).
- Dimensional deviation and surface roughness are given equal significance, while material removal rate is disregarded ($w_{\Delta d} = w_{Ra}$ and $w_{MRR} = 0$).
- Dimensional deviation and material removal rate are assigned equal importance, while surface roughness is disregarded ($w_{\Delta d} = w_{Ra}$ and $w_{MRR} = 0$).
- Surface roughness and material removal rate are given equal importance, while dimensional deviation is disregarded ($w_{\Delta d} = w_{Ra}$ and $w_{MRR} = 0$).

The results obtained from these cases are presented in Table 10.

3.4 Results from Confirmation Experiments

Modelling and optimization verification were carried out through four additional confirmation experiments. These experiments aimed to verify the accuracy and reliability of the developed model, as well as to assess the effectiveness of the optimized parameters under real conditions. The results obtained, along with the calcu–lated errors, are presented in Tables 11 and 12.

Table 10. Optimization results

Weighting coefficients	Input variables		Output variables
$w_{\Delta d}=w_{Ra}=w_{MRR}$	v_c (m/s) = 25 v_w (m/s) = 0.2 f (mm/rev) = 25 Δ (mm) = 0.34	i = 4 WGS = Fine WP = Medium	Δd (mm)=0.0064 Ra (μm)=0.5396
$w_{\Delta d}=w_{Ra}$, $w_{MRR}=0$	v_c (m/s) = 28.2 v_w (m/s) = 0.2 f (mm/rev) = 12.5 Δ (mm) = 0.12	i = 8 WGS = Fine WP = Medium	Δd (mm)=0.0046 Ra (μm)=0.4619
$w_{\Delta d}=w_{MRR}$, $w_{Ra}=0$	v_c (m/s) = 25 v_w (m/s) = 0.2 f (mm/rev) = 25 Δ (mm) = 0.36	i = 4 WGS = Fine WP = Medium	Δd (mm)=0.0063 Ra (μm)=0.5418
$w_{Ra}=w_{MRR}$, $w_{\Delta d}=0$	v_c (m/s) = 35 v_w (m/s) = 0.2 f (mm/rev) = 25 Δ (mm) = 0.36	i = 4 WGS = Fine WP = Porous	Δd (mm)=0.0112 Ra (μm)=0.5037

Table 11. Results of confirmation experiments for Δd

Weighting coefficients	v_c (m/s)	v_w (m/s)	f (mm/rev)	Δ (mm)	i	WGS	WP	Δd (mm) measured	Δd (mm) predicted	$AE_{\Delta d}$ (mm)
$w_{\Delta d}=w_{Ra}=w_{MRR}$	25	0.2	25	0.34	4	Fine	Medium	0.0069	0.0064	0.0005
$w_{\Delta d}=w_{Ra}$, $w_{MRR}=0$	28.2	0.2	12.5	0.12	8	Fine	Medium	0.0050	0.0046	0.0004
$w_{\Delta d}=w_{MRR}$, $w_{Ra}=0$	25	0.2	25	0.36	4	Fine	Medium	0.0069	0.0063	0.0006
$w_{Ra}=w_{MRR}$, $w_{\Delta d}=0$	35	0.2	25	0.36	4	Fine	Porous	0.0122	0.0112	0.001

Table 12. Results of confirmation experiments for Ra

Weighting coefficients	v_c (m/s)	v_w (m/s)	f (mm/rev)	Δ (mm)	i	WGS	WP	Ra (μm) measured	Ra (μm) predicted	AE_{Ra} (μm)
$w_{\Delta d}=w_{Ra}=w_{MRR}$	25	0.2	25	0.34	4	Fine	Medium	0.5498	0.5396	0.0102
$w_{\Delta d}=w_{Ra}$, $w_{MRR}=0$	28.2	0.2	12.5	0.12	8	Fine	Medium	0.4842	0.4619	0.0223
$w_{\Delta d}=w_{MRR}$, $w_{Ra}=0$	25	0.2	25	0.36	4	Fine	Medium	0.5642	0.5418	0.0224
$w_{Ra}=w_{MRR}$, $w_{\Delta d}=0$	35	0.2	25	0.36	4	Fine	Porous	0.5282	0.5037	0.0245

4. DISCUSSION

The ANOVA analysis results for both evaluated responses (Δd and Ra) indicate that the models exhibit extremely high F-test values—3 871.824 for Δd and 110 680.4 for Ra - along with very low p-values (less than 0.0001). This demonstrates that the models are statistically significant with a high level of confidence, meaning that the independent variables and their interactions significantly influence the system's responses. These findings validate the developed models and support their further use in analysing and optimizing the grinding process.

The results presented in the summary of fit show high values for the coefficient of determination (Rsquare) of 0.999338 for Δd and 0.999977 for Ra, indicating that the models successfully explain approximately 99% of the variance in the experimental data. The adjusted coefficient of determination (RSquare Adj) is also high, with values of 0.999079 for Δd and 0.999968 for Ra, confirming the stability and reliability of the models even after accounting for model complexity. Additionally, the root mean square error values are very low, measuring at 6.613e-5 for Δd and 0.007013 for Ra. This indicates a small average prediction error, which further confirms the high precision of the models. When compared to the mean response values of 0.008927 for Δd and 1.840204 for Ra, these errors are negligible, further supporting the overall quality of the models.

Results from k-fold cross-validation (with k=10) confirm that the models are not overfitted to the training data's specific characteristics and demonstrate good generalization capabilities for new, unseen data. This method significantly reduces bias in estimating model performance, providing a more reliable assessment of their quality. Additionally, model stability is confirmed through statistical tests and visual representations, which indicate their robustness and practical value for further application in industrial conditions.

Summary of fit results for the one-way ANOVA of residuals shows that for Ra, the RSquare value is 0.1117, while the RSquare Adj is 0.0301. This indicates that only a small portion of the residual variance can be explained by grouping into validation folds. Similarly, for Δd, the RSquare is 0.0750, and the RSquare Adj is negative (-0.0100), suggesting negligible explanatory power from grouping by folds.

Based on the F-test and p-values ($F = 0.8828$, $p = 0.5434$ for Δd; $F = 1.3689$, $p = 0.2127$ for Ra) from the one way ANOVA, no statistically significant differences were observed between the validation groups. This reflects the homogeneity of residual values and the strong predictive capability of the models across different data subsets.

Based on the prediction profilers, the following conclusions can be drawn:

- Dimensional deviation decreases when the wheel speed, workpiece speed, feed, and total depth of cut are reduced, while it increases with the number of passes. Additionally, dimensional deviation is lowest when using a fine wheel grain size and medium wheel porosity.
- Surface roughness decreases with increasing wheel speed and decreasing workpiece speed, feed, and total depth of cut, while it also improves with more passes. Furthermore, the smallest surface roughness is observed with fine wheel grain sizes and porous wheel porosity.

Dimensional deviation and surface roughness tend to decrease with increasing wheel speed and workpiece speed. This occurs because a faster wheel grinds the workpiece surface with more abrasive grains, resulting in a smoother finish and reduced surface roughness. However, at higher speeds, the cutting forces also increase, leading to more heat generation and intensified wear, which contribute to increased dimensional deviation.

Conversely, dimensional deviation and surface roughness increase with an increase in feed. A larger feed means the wheel moves more quickly across the workpiece surface, removing less material and leaving higher peaks and valleys. This situation worsens surface roughness. Additionally, as the feed rate increases, the cutting forces rise, heat generation increases, and wear intensifies, further reducing dimensional accuracy.

Dimensional deviation and surface roughness decrease when the total depth of cut and the number of passes are reduced. A smaller total depth of cut and fewer passes result in a shallower depth of cut (total depth of cut/number of passes). This reduction leads to lower cutting forces, less heat generated in the cutting zone, and minimized tool wear. Consequently, both dimensional accuracy and surface roughness improve.

Moreover, smaller grain sizes contribute to reduced dimensional deviation and surface roughness. Fine grinding wheels, due to their smaller grains, create a greater number of contact points, which reduces the cutting force, heat, and wear. This results in a more uniform scratch pattern and lower peak and valley heights, enhancing dimensional accuracy and decreasing surface roughness.

Lastly, surface roughness decreases as the porosity of the wheel increases. Higher porosity in grinding wheels leads to lower cutting forces, improved heat dissipation, and more uniform wear. However, while more porous wheels sharpen themselves more frequently, optimal dimensional accuracy is typically observed with wheels of medium porosity, as they balance performance better than both dense and overly porous structures.

The interaction profiler analysis reveals that the influence of input variables on Δd and Ra depends on their mutual interactions rather than solely on their individual effects. The behaviour of the output variables cannot be fully explained by isolated effects of single factors; instead, it changes depending on their combination. For both output variables, multiple statistically significant interactions were identified, with particularly pronounced effects observed between the grinding wheel grain size and other process parameters, as well as between the total depth of cut and the number of passes.

For surface roughness, it was observed that the effects of parameters such as wheel speed, workpiece speed, feed, total depth of cut, and number of passes are less pronounced when a grinding wheel with finer grit is used. This suggests that fine grains dampen roughness variations caused by changes in these parameters, due to more uniform material removal and lower localized stresses.

Furthermore, increasing the number of passes reduces the influence of total depth of cut on both *Ra* and Δd. A higher number of passes means that the same amount of material is removed in multiple thin layers, resulting in lower cutting forces per pass, better process control, and more stable output results.

In the case of dimensional deviation, it was found that grit size does not have a decisive impact on the system's sensitivity to changes in input variables. In other words, regardless of whether coarse or fine grains are used, the effects of wheel speed, workpiece speed, feed, depth of cut, and number of passes on Δd remain approximately the same.

Optimization results indicate that, regardless of the significance of the output variables (their weighting coefficients), two input variables consistently appear in the optimal combinations: the minimum level of work–piece speed and fine grain size. This is because low workpiece speed and fine grain size lead to the most accurate machining (i.e., the lowest dimensional devi–ation) and the best surface quality (i.e., the lowest sur–face roughness), while having no significant impact on *MRR*. The remaining input variables vary depending on the specific case.

In the first case, wheel speed is at its minimum level, feed is at its maximum, total depth of cut is close to its maximum, number of passes is at its minimum, and wheel porosity is medium. This is due to the fact that feed, total depth of cut, and number of passes directly affect *MRR* but do not have a significant negative impact on Δd and *Ra*. Additionally, wheel speed is kept low because it has a greater positive effect on dimen–sional deviation than a negative effect on surface rough–ness. Furthermore, medium wheel porosity yields the best dimensional accuracy with only a slight reduction in surface quality.

In the second case, wheel speed is close to its minimum, feed is at its minimum, total depth of cut is at its minimum, number of passes is at its maximum, and wheel porosity is medium. This is because a low feed, low depth of cut, and high number of passes result in the lowest dimensional deviation and the lowest surface roughness. Additionally, the wheel speed remains close to its minimum because of its more favourable influence on dimensional deviation than its adverse effect on *Ra*. Again, medium wheel porosity provides the best dimen–sional control with slightly reduced surface finish.

In the third case, wheel speed is at its minimum, feed is at its maximum, total depth of cut is at its maxi–mum, number of passes is at its minimum, and wheel porosity is medium. This configuration is effective be–cause feed, total depth of cut, and number of passes directly influence *MRR* without significantly affecting Δd. Moreover, the minimum wheel speed and medium porosity contribute to the lowest dimensional deviation.

In the fourth case, wheel speed is at its maximum, feed is at its maximum, total depth of cut is at its maxi–mum, number of passes is at its minimum, and wheel porosity is high (porous). This is because feed, depth of cut, and number of passes directly affect *MRR* but have little negative effect on *Ra*. Additionally, the maximum wheel speed and porous wheel structure result in the lowest surface roughness.

The results of confirmation experiments validate the accuracy of the modelling and optimization approach. The absolute errors for dimensional deviation ranged between 0.0004–0.001 mm, with a mean absolute error of 0.000625 mm. The absolute errors for surface rough–ness ranged between 0.0102–0.0245 μm, with a mean absolute error of 0.019850 μm. These absolute errors are negligible under practical conditions, indicating that the developed methodology can be effectively applied in real manufacturing environments.

5. CONCLUSION

This study presents a comprehensive multi-objective optimization of the external cylindrical longitudinal grinding process for the AISI 6150 steel alloy. The goal was to optimize dimensional accuracy, surface quality, and productivity simultaneously. The effects of seven input variables - grinding wheel speed, workpiece speed, feed rate, total depth of cut, number of passes, grain size, and grinding wheel porosity—were analysed using a customized experimental design.

Using an I-optimal experimental design and multiple regression analysis, we developed reliable statistical models that demonstrate exceptional accuracy (RSquare > 0.999). We confirmed their stability through ANOVA tests, cross-validation, and experimental verification. The findings indicate that all seven input variables significantly influence process performance. Interaction analysis showed that the number of passes, total depth of cut, and grain size, when interacting with other factors, have a substantial impact on the quality and accuracy of the grinding. Therefore, successful optimi–zation must consider not only the individual effects of each variable but also their interdependencies to achieve a balanced compromise between process requirements.

The proposed approach improves process planning and quality control in grinding operations. The developed models and optimization framework can be directly implemented in production systems using external cylin–drical longitudinal grinding as a finishing operation. The resulting models and optimized solutions demonstrate high accuracy and stability, making them well suited to indus–trial applications. They enable reliable prediction of key performance indicators, reduce the need for trial-and-error adjustments, and support efficient selection of grinding and wheel parameters in the production of high-precision workpieces. Furthermore, the multi-objective optimization framework allows flexible selection of grinding and wheel parame–ters according to specific production priorities.

However, the current model's applicability is limited to the specific conditions under which the experiments were conducted. To improve its versatility and accu–racy, future research will focus on expanding the model by incorporating additional input and output variables. This enhancement will enable better adaptation to varying process conditions.

REFERENCES

[1] Rowe, W.B., Yan, L., Inasaki, I. Malkin, S.: Applications of Artificial Intelligence in Grinding, CIRP Annals, Vol. 43, No. 2, pp. 521-531, 1994.

[2] Deepanraj, B., Raman, L.A., Senthilkumar, N. and Shivasankar, J.: Investigation and Optimization of Machining Parameters Influence on Surface Roughness in Turning AISI 4340 Steel, FME Transactions, Vol. 48, No. 2, pp. 383-390, 2020.

[3] Chtioui, A., Ouballouch, A. and Mouchtachi, A.: Investigation of Cutting Responses During High-speed Machining of Ti6Al4V Alloy: Finite Element Analysis, FME Transactions, Vol. 52, No. 4, pp. 616-627, 2024.

[4] Meng, Q., Guo, B., Zhao, Q., Li, H.N., Jackson, M.J., Linke, B.S. Luo, X.: Modelling of grinding mechanics: A review, Chinese Journal of Aero–nautics, Vol. 36, No. 7, pp. 25-39, 2023.

[5] Saric, T., Simunovic, G., Vukelic, D., Simunovic, K., Lujic, R.: Estimation of CNC Grinding Process Parameters Using Different Neural Networks, The–nicki vjesnik–Technical Gazette, Vol. 25, No. 6, pp. 1770-1775, 2018.

[6] Kishore, K., Sinha, M.K., Singh, A., Archana, Gupta, M.K., Korkmaz, M.E.: A comprehensive re–view on the grinding process: advancements, appli–cations and challenges, Proceedings of the Insti–tution of Mechanical Engineers, Part C: Journal of Mechanical Engineering Science, Vol. 236, No. 22, pp. 10923-10952, 2022.

[7] Lv, L., Deng, Z., Liu, T., Li, Z., Liu, W.: Intelligent technology in grinding process driven by data: A review. Journal of Manufacturing Processes, Vol. 58, pp. 1039-1051, 2020.

[8] Chowdhury, M.A.K., Rehman, A.U., Uddin, M.S., Alkahtani, M., Anwar, S.: Multi Criteria Optimi–zation Approach for Dressing of Vitrified Grinding Wheel, Tehnicki vjesnik–Technical Gazette, Vol. 25, Supplement 2, pp. 256-265, 2018.

[9] Rekha, R., Vinoth Kumar, S., Aravinth Raj, V., Aswin Baboo, B., Gokul Raj, P., Jai Vignesh, A.: Optimization of cylindrical grinding process para–meters on austenitic stainless steel 304 using Ta–guchi based Grey Relational Analysis, Materials Today: Proceedings, Vol. 72, pp. 2569-2573, 2023.

[10] Kara, F., Koklu, U., Kabasakaloglu, U.: Taguchi optimization of surface roughness in grinding of cryogenically treated AISI 5140 steel, Materials Testing, Vol. 62, No. 10, pp. 1041-1047, 2020.

[11] Rudrapati, R., Bandyopadhyay, A., Pal, P.K., Rathod, L.: Analysis, modeling and optimization of surface roughness in cylindrical traverse cut grinding using factorial design, RSM and simulated annealing algorithm, IOP Conference Series: Materials Science and Engineering, Vol. 814, 012016, 2020.

[12] Chi, Y.L., Li, H.L., Cao, H.Y., Lin, X.K.: Grinding Parameters Optimization of Stainless Steel Surface Based on Grey Relational Analysis, Advanced Ma–terials Research, Vol. 690-693, pp. 2450-2455, 2013.

[13] Hong, T.T., Hoang, X.T., Ky, L.H., Nguyen, Q.T., Nguyen, T.T., Nga, N.T.T., Jun, G., Pi, V.N.: A Study on Cost Optimization of External Cylindrical Grinding, Materials Science Forum, Vol. 977, pp. 18-26, 2020.

[14] Panthangi, R.K., Naduvinamani V.: Optimization of surface roughness in cylindrical grinding pro–cess, International Journal of Applied Engineering Research, Vol. 12, No. 18, pp. 7350-7354, 2017.

[15] Trung, D.D., Quang, N.H., Cuong, D.Q., Linh, N.H., Tuan, N. Van., Hung, L.X., Tuan, N.A.: Combining Taguchi method and DEAR method for multi-objective optimization of grinding process, E3S Web of Conferences, Vol. 309, 01220, 2021.

[16] Gopan, V., Wins, K.L.D., Surendran, A.: Integrated ANN-GA Approach for Predictive Modeling and Optimization of Grinding Parameters with Surface Roughness as the Response, Materials Today: Pro–ceedings, Vol. 5, No. 5, pp. 12133-12141, 2018.

[17] Nguyen, A.T., Nguyen, T.T.N., Tran, Q.H., Nguyen, H.Q., Le, H.A., Nguyen, H.L., Tran, N.G. Hoang, X.T.: Multi-objective Optimization for Mi–nimum Surface Roughness and Maximum Wheel Life When External Cylindrical Grinding SKD11 Steel, Advances in Engineering Research and Application, pp. 601-609, 2022.

[18] Nguyen, T.L.: Modeling of external cylindrical grinding process using T1 tool steel, EUREKA: Physics and Engineering, Vol. 3, pp. 85-98, 2021.

[19] Jadhav, P., Patil, P., Patil, S.: Optimization of Cy–lindrical Grinding for Material Removal Rate of Alloy Steel EN9 by Using Taguchi Method, Ad–vances in Industrial and Production Engineering, pp. 851-859, 2021.

[20] Kumar Patel, D., Goyal, D., Pabla, B.S.: Optimi–zation of parameters in cylindrical and surface grinding for improved surface finish, Royal Society Open Science, Vol. 5, No. 5, 171906, 2018.

[21] Alsigar, M., Pereverzev, P., Almawash, A., Alkadhim, M.: Optimal design of grinding systems with use of mathematical complex models ECGA, Materials Today: Proceedings, Vol. 38, pp. 1521-1525. 2021.

[22] Tien D.H., Trung D.D., Thien N.V., Nguyen N.T.: Multi-objective optimization of the cylindrical grinding process of SCM440 steel using Preference Selection Index Method, Journal of Machine Engineering. Vol. 21, No. 3, pp. 110-123, 2021.

[23] Rudrapati, R., Pal, P.K. and Bandyopadhyay, A.: Modeling and optimization of machining para–meters in cylindrical grinding process, International Journal of Advanced Manufacturing Technology, Vol. 82, No. 9-12, pp. 2167-2182, 2015.

[24] Gangmei, G., Chawang, M., Tamang, S.K., Chandrasekaran, M.: Fuzzy set based optimization for grinding Al/SiC MMC; an approach to maxi–mize MRR satisfying desired surface roughness, International Journal of Modern Manufacturing Technologies, Vol. 10, No. 1, pp. 43-49, 2018.

[25] Giang, T.N., Bui, K.K., Dang, Q.C., Nguyen, D.N., Hoang, X.T. and Pi, V.N.: Studying the Influence of Dressing Parameters on the Surface Roughness when Conducting the External Grinding of SKD11 Steel, Solid State Phenomena, Vol. 324, pp. 45-51, 2021.

[26] Ding, Z., Jiang, X., Guo, M., Liang, S.Y.: Investi–gation of the grinding temperature and energy partition during cylindrical grinding, International Journal of Advanced Manufacturing Technology, Vol. 97, No. 5-8, pp. 1767-1778, 2018.

[27] Rekha, R., Baskar, N., Padmanaban, K., Venka–traman, V.: Application of regression analysis and evolutionary algorithms for modeling and optimi–zation of cylindrical grinding process parameters for the prediction of surface roughness of AISI 316, International Journal of Applied Engineering Research, Vol. 10, No. 5, pp. 12593-12610, 2015.

[28] Neseli, S., Asilturk, I., Celik, L.: Determining the optimum process parameter for grinding operations using robust process, Journal of Mechanical Sci–ence and Technology, Vol. 26, No. 11, pp. 3587-3595. 2012.

ACKNOWLEDGMENT

This research has been supported by the Ministry of Science, Technological Development and Innovation of the Republic of Serbia, and the Faculty of Technical Sciences, University of Novi Sad through project "Scientific and Artistic Research Work of Researchers in Teaching and Associate Positions at the Faculty of Technical Sciences, University of Novi Sad". Also, this research paper was funded by the University of Slavonski Brod through the institutional research project Advanced Modeling and Optimization of Compact Heat Exchangers for Integration into Renewable Energy Systems (MOKIT), financed by the European Union – NextGenerationEU. The views and opinions expressed in this paper are those of the author and do not necessarily reflect the official position of the European Union or the European Commission. Neither the European Union nor the European Commission can be held responsible for them.

NOMENCLATURE

a_p	Depth of cut
B	Grinding wheel width
D	Grinding wheel diameter
d	Grinding wheel hole
d_{2m}	Measured value of the diameter after grinding
d_{1n}	Measured diameter value before grinding
d_{2n}	Required - nominal value of the diameter after grinding
f	Feed
F_c	Objective function
i	Number of passes
Ra	Surface roughness
v_c	Wheel speed
v_w	Workpiece speed
w	Weighting coefficient of the output variable
x	Normalized value of the output variable
Δ	Total depth of cut
Δd	Dimensional deviation

Acronyms and Abbreviations

AE	Absolute Error
ANN	Artificial Neural Network
ANOVA	Analysis of Variance
DF	Degrees of Freedom
GA	Genetic Algorithm
MRR	Material Removal Rate
PSI	Preference Selection Index
PSO	Particle Swarm Optimization
RSM	Response Surface Methodology
SA	Simulation Annealing
WGS	Wheel grain size
WP	Wheel porosity

ОПТИМИЗАЦИЈА ПАРАМЕТАРА БРУШЕЊА И ТОЦИЛА ТОКОМ СПОЉАШЊЕ ЦИЛИНДРИЧНЕ УЗДУЖНЕ ОБРАДЕ ЛЕГИРАНОГ ЧЕЛИКА AISI 6150 НА ОСНОВУ ТАЧНОСТИ, КВАЛИТЕТА И ПРОДУКТИВНОСТИ

А. Милошевић, В. Иванов, С. Шимуновић, Ђ. Вукелић

У истраживању је спроведена вишекритеријумска оптимизација процеса спољашњег цилиндричног уздужног брушења легираног челика AISI 6150. Улазне промењљиве чији је утицај испитиван су брзина тоцила, брзина обратка, помак, укупни до–датак за обраду, број пролаза, величина зрна тоцила и порозност тоцила. Експериментално истраживање је спроведено коришћењем прилагођеног дизајна експеримента заснованог на И-критеријуму опти–малности. Димензионо одступање је изабрано за квантификацију тачности, храпавост површине за процену квалитета, а брзина уклањања материјала за мерење продуктивности. Вредности димензионог одступања су биле од 0,0046 до 0,0144 mm, вредности храпавости површине су биле између 0,4301 и 3,766 μm, а брзина уклањања материјала је била од 9,375 до 112,5 mm³. На основу експе–риментаних резултата, спроведена је анализа како би се дефинисао утицај улазних на излазне про–менљиве и развијене су регресионе једначине. Циљ је био истовремена оптимизација тачности, ква–литета и продуктивности, уз варирање тежинских коефицијената у функцији циља. Поузданост модела и оптималне вредности промењљивих потврђене су кроз конфирмационе експерименте. Добијене апсо–лутне грешке биле су прихватљиве, и износе 0,0004 и 0,001 mm за димензионо одступање и 0,0102 до 0,0245 μm за храпавост површине.